AN EXPERIMENTAL INVESTIGATION ON THE DEFORMATION OF FONTAINEBLEAU SANDSTONE

J. Fonseca[1], Z. Karatza[2], P. Bésuelle[2] and G. Viggiani [2]

[1] School of Engineering and Mathematical Sciences, City University London, UK
[2]Grenoble-INP, UJF-Grenoble 1, CNRS UMR 5521, Laboratoire 3SR, France

1. INTRODUCTION

Sandstones constitute an economically and geologically important class of geomaterials. Predicting changes in physical properties of these rocks in response to varying in-situ conditions is at the core of many geotechnical problems, e.g., oil prospecting, development of geothermal energy, assessment of suitability for underground repositories for CO2 and radioactive nuclear waste. Understanding the evolution of the microstructure with loading is fundamental to predict the response of soil and provide relevant parameters to describe soil behaviour, e.g. [1] and [2]. The present study investigates the microscale mechanisms occurring on specimens of sandstone loaded to failure by means of x-ray computed tomography (micro-CT). The evolution in the internal topology of the material is linked to the macro scale response given by the stress and strain variables. Strains are measured using a full field technique [3] which allows a more accurate interpretation of the effect of heterogeneity in the specimen as a consequence of localisation, when compared to more conventional measurements using transducers.

2. METHODOLOGY

Intact specimens of Fontainebleau sandstone, a quartzite formation from the Paris Basin (France) were investigated. An outstanding characteristic of this formation is the contrast between the very hard, tightly cemented sandstone and the more porous and less cemented material, without noticeable grain size modification [4]. The specimens used for this study had porosities 6% (designed as 'stiff sandstone' hereafter) and 21% ('soft sandstone'). Triaxial compression tests were performed in a small high-pressure triaxial cell designed to operate inside the x-ray scanner, which allows scanning at the same time as loading. The triaxial specimens were 22mm high and 11mm in diameter and the 3D images of the full specimen were acquired at key stages throughout deformation. Confining pressures of 2MPa and 7MPa were used and the deviatoric loading was applied by an ascending piston at a rate of 21μm/min. The acquired images have a spatial resolution of 8.5μm which means that the diameter of a median size grain is represented by approximately 30 voxels. This level of detail has permitted to identify geometrical rearrangement of grains and to trace the development of grain cracks (for cracks aperture greater than 8.5μm) as reported in [5]. The present work takes the grain-level investigation forward by providing an analysis of the evolutions of macro strains measured from the tomographic images. The values of axial strain were obtained by measuring the shortening of the specimen in the image for subsequent loading stages, using the same reference points for different stages. The volumetric strain was inferred from the total number of the voxels defining the specimen, which includes void voxels and solid or grain voxels located within the membrane of the triaxial specimen. Image processing techniques were developed to obtain a good definition for this boundary. The outlining of the specimen was also used for the radial strain calculation. In order to take into account the possible deviations of the cross section of the specimen from the initial circular shape, the average of 10 measurements passing through the centroid, on a spectrum of 180º, was used.

3. OBSERVATIONS

The results on three of the seven specimens tested are presented here. This includes a soft specimen tested at 7MPa FBS02-7MPa, a soft specimen tested at 2MPa (FBS03-2MPa) and a stiff specimen tested at 2MPa (FBH01-2MPa). The mechanical response is presented in the plot of deviatoric stress against axial strain (obtained from external transducer), Figure 1a. The three samples exhibit brittle behavior and the peak stress value is a function of both the degree of cement and the confining pressure. The soft specimens failed along a well defined shear band with an orientation angle, with respect to the minor principal stress, of 53º and of 48º for the tests at 2MPa and 7MPa, respectively. The stiff sandstone exhibited a more complex failure mode with a combination of axial splitting and multiple shear bands. Figure 1b shows the evolution of the volumetric and radial strain against axial strain, all measured directly from the images. The strains were calculated with reference to the initial dimensions of the specimen, therefore, they comprise deformation from both isotropic compression and shearing stages. Although the axial strain in Figure 1a refers only to the shearing stage and cannot be compared with Figure 1b, it has been observed that the measurements from the external transducer tend to overestimate the axial shortening of the specimen and this is more pronounced for the soft material tested at lower confining pressure. The analysis of the volumetric strain shows that the soft specimens initially contract from stage 0 to stage 2, suggesting that during this period the stressed lithified contacts underwent disruption which allowed the unbounded grains to rearrange and the specimen to start to dilate as observed from stage 2. The increase in volumetric strain is more significant for the sample FBS03-2MPa and this is in agreement with the large voids that were observed in the shear band of this sample from the tomographic images; while the almost zero volumetric strain of the sample FBS02-7MPa at the end of the test is a consequence of the intense grain breakage, crushing and porosity reduction observed in the shear plane of this specimen. The evolution of the radial strain shows that specimen FBS02-7MPa contracts radially up to stage 2, contrary to the soft sample tested at lower confining pressure. The radial contraction of the specimen FBS02-7MPa suggests that for higher confining pressures the grains are unbonded both in the horizontal and vertical directions. This fact can greatly influence the damage mechanisms and also be related to the different inclination of the shear plane for specimens FBS02-7MPa and FBS03-2MPa. Regarding the stiff material, the confining pressure of 2MPa is not significant to disrupt the tight cement and the initial dilation of the specimen suggests the onset of a localized deformation that leads to the axial splitting that occurs between stage 2 and 3 (indicated by the small plateau in the stress:strain curve just before stage 3). The large volumetric strain measured for the stiff specimen is a result of a complex failure phenomena associated with the formations of large voids in the regions where rupture of cement between grains occurs in the direction of the major principal stress and the collapse of vertical columns of horizontally unbounded grains [5].

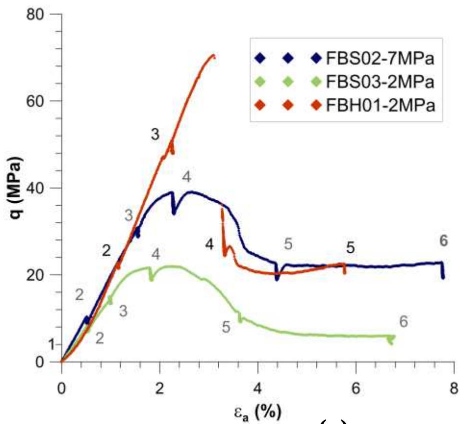

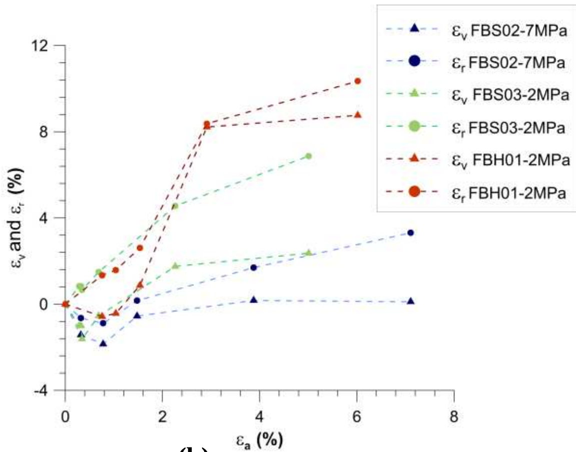

Figure 1. (a) Deviatoric stress against axial strain with indication of the loading stages chosen for imaging (marked by small relaxations in the stress deviator) and **(b)** Evolution of volumetric strain and radial strain against axial strain (measured from the tomographic images)

3. CONCLUSION

Full field measurements are used in this study as part of an investigation into the damage mechanisms of Fontainebleau Sandstone during deformation to failure. Unlike cohesionless materials, the lithified contacts of this sandstone prevent any contraction or dilation to occur unless the loss in contact cohesion is sufficient the cause grains to rearrange either by slip or rotation or to break. The data on the strain evolution provides additional insights into the inter and intra-granular cracking observed in the tomographic images [5]. The transition from the initial volumetric contraction to dilation exhibited by the soft specimens suggests that localized topological changes have initiated following an initial disruption of the bonding between grains. This indicates that localization is initiated well before peak is attained regardless of the fact that it only becomes visible in the post-peak regime. The analysis of the radial strain evolution sheds a light on the effect of confining pressure on the rupture of the cement and consequently on the progress of the localization phenomena including the inclination of the shear band.

References

[1] Fonseca, J., O'Sullivan, C., Coop, MR., Lee, P.D. Quantifying the evolution of soil fabric during shearing using scalar parameters. Géotechnique, 63, No. 10, pp. 818-829, 2013

[2] Menéndez, B., Zhu, W., Wong, T.-F. Micromechanics of brittle faulting and cataclastic flow in Berea sandstone. Journal of Structural Geology, 18, pp. 1-16, 1996

[3] Viggiani, G., Hall, S. A. Full-field measurements, a new tool for laboratory experimental geomechanics. In Proc. of the 4th Int. Symposium on Deformation Characteristics of Geomaterials (Burns SE, Mayne PW and Santamarina JC (Eds.)) pp. 3-26, 2008

[4] Thiry, M., Marechal, B., Development of Tightly Cemented Sandstone Lenses in Uncemented Sand: Example of the Fontainebleau Sand (Oligocene) in the Paris Basin. Journal of Sedimentary Research, 71, No. 3, pp. 473-483, 2001

[5] Fonseca, J., Bésuelle, P., Viggiani, G. Micromechanisms of inelastic deformation in sandstones: an insight using x-ray micro-tomography. Géotechnique Letters 3, No. 2, pp. 78–8, 2013